Science Advances
AAAS

advances.sciencemag.org/cgi/content/full/6/15/eaaw0158/DC1

Supplementary Materials for

Soft extracellular matrix enhances inflammatory activation of mesenchymal stromal cells to induce monocyte production and trafficking

Sing Wan Wong, Stephen Lenzini, Madeline H. Cooper, David J. Mooney*, Jae-Won Shin*

*Corresponding author. Email: mooneyd@seas.harvard.edu (D.J.M.); shinjw@uic.edu (J.-W.S.)

Published 8 April 2020, *Sci. Adv.* **6**, eaaw0158 (2020)
DOI: 10.1126/sciadv.aaw0158

This PDF file includes:

Mathematical modeling

TNFα-mediated NF-κB activation

The fraction of an interacting protein X bound to a target Y is generally described by a standard Hill function:

$$\theta_X^Y = \frac{1}{1 + \left(\frac{K_X^Y}{[X]}\right)^n} \qquad (Eq. 1.1).$$

K_X^Y is the concentration of X where the total bound protein complex is half-maximum (***potency***). n denotes cooperativity of binding, which is typically 1 or 2 (*25*).

θ_X^Y is used to describe stimulation upon binding, while $1 - \theta_X^Y$ is used to describe repression.

We constructed a set of differential equations to describe the kinetics of NF-κB activation (phosphorylated p65) in response to TNFα binding to TNF receptor (TNFR). We implemented an incoherent feedforward loop (I1-FFL) where TNFR stimulation leads to NF-κB activation and induction of factors that in turn inhibit activated NF-κB (**Fig. S2C**).

$$\frac{dI}{dt} = \beta_I \theta_{TNF\alpha}^{TNFR} - \alpha_I I \qquad (Eq. 1.2)$$

where *I* is the concentration of factors that are induced upon TNFR stimulation, which subsequently inhibit activated NF-κB (deemed 'inhibitors'). β_I is the intrinsic or constitutive production rate of *I*. $\theta_{TNF\alpha}^{TNFR}$ denotes dose response for stimulation of TNFR by TNFα (*Eq*. 1.1). α_I is the decay rate of *I*.

$$\frac{dpNF}{dt} = \beta_{pNF} \theta_{TNF\alpha}^{TNFR} (1 - \theta_I^{pNF}) - \alpha_{pNF} pNF \qquad (Eq. 1.3)$$

,where *pNF* is the concentration of activated NF-κB. β_{pNF} is the intrinsic or constitutive production rate of *pNF*. $1 - \theta_I^{pNF}$ denotes dose response for repression of *pNF* by *I*. Both

stimulated TNFR and *I* determine *pNF*, and hence their functions are multiplied (*25*). α_{pNF} is the decay rate of *pNF*.

Analytical solution of *Eq.* 1.3 leads to:

$$pNF = \frac{\beta_{pNF}}{\alpha_{pNF}}\theta_{TNF\alpha}^{TNFR}(1-\theta_I^{pNF}) + Ce^{-\alpha_{pNF}t} \qquad (Eq.1.4)$$

At t = 0,

$$pNF_0 = \frac{\beta_{pNF}}{\alpha_{pNF}}\theta_{TNF\alpha}^{TNFR}(1-\theta_I^{pNF}) + C \qquad (Eq.1.5)$$

Substituting Eq. 1.5 into Eq. 1.4, followed by rearrangement leads to:

$$pNF = \frac{\beta_{pNF}}{\alpha_{pNF}}\theta_{TNF\alpha}^{TNFR}(1-\theta_I^{pNF})(1-e^{-\alpha_{pNF}t}) + pNF_0e^{-\alpha_{pNF}t} \qquad (Eq.1.6)$$

The maximum level of *pNF* (pNF_m) occurs when the inhibition is 0, i.e. $(1-\theta_I^{pNF}) = 1$, and t = ∞. Thus,

$$pNF_m = \frac{\beta_{pNF}}{\alpha_{pNF}}\theta_{TNF\alpha}^{TNFR} \quad (Eq.1.7).$$

The equation for the fold change in *pNF* is:

$$F_{pNF} = \frac{pNF}{pNF_0} = F_{pNF_m}(1-\theta_I^{pNF})(1-e^{-\alpha_{pNF}t}) + e^{-\alpha_{pNF}t} \qquad (Eq.1.8)$$

where $F_{pNF_m} = \frac{pNF_m}{pNF_0}$.

Assuming that the initial level of *I* is very low (~0) (*42*, *43*), solving Eq. 1.2 leads to:

$$I = \ I_{st}\,(1 - e^{-\alpha_I t}) \quad (Eq.\,1.9)$$

where $I_{st} = \frac{\beta_I}{\alpha_I}\theta_{TNF\alpha}^{TNFR}$.

Substituting Eq. 1.9. into Eq 1.8., leads to:

$$F_{pNF} = F_{pNF_m}(1 - \frac{1}{1 + \left(\frac{K_I^{pNF}}{I_{st}(1-e^{\alpha_I t})}\right)^n})(1 - e^{-\alpha_{pNF} t}) + \ e^{-\alpha_{pNF} t} \qquad (Eq.\,1.10)$$

In a simple case when n = 1, rearranging Eq. 1.10 leads to:

$$F_{pNF} = F_{pNF_m}(\frac{I_{ratio}}{I_{ratio} + (1 - e^{\alpha_I t})})(1 - e^{-\alpha_{pNF} t}) + \ e^{-\alpha_{pNF} t} \qquad (Eq.\,1.11)$$

, where $I_{ratio} = \frac{K_I^{pNF}}{I_{st}}$

At the steady state ($F_{pNF_{st}}$), t = ∞,

$$F_{pNF_{st}} = F_{pNF_m}\left(\frac{I_{ratio}}{I_{ratio} + 1}\right) \quad (Eq.\,1.12)$$

The maximum to steady state ratio of *pNF* (R) = $\frac{F_{pNF_m}}{F_{pNF_{st}}} = \ \frac{pNF_m}{pNF_{st}}$ is constant because:

$\frac{soft\ pNF_m}{stiff\ pNF_m} = \frac{soft\ pNF_{st}}{stiff\ pNF_{st}}$ = ~1.6 when t ≥ 10 min after TNFα stimulation (**Fig. S2B**),

$$I_{ratio} = \left(\frac{1}{R - 1}\right) \quad (Eq.\,1.13).$$

Finally, substituting Eq. 1.13 to Eq. 1.11, and rearrangement leads to:

$$F_{pNF} = F_{pNF_m} \frac{1 - e^{-\alpha_{pNF}t}}{1 + (1 - e^{\alpha_I t})(R - 1)} + e^{-\alpha_{pNF}t} \qquad (Eq. 1.14)$$

; Hence, β_I no longer exists in this equation. pNF_0 is similar between soft and stiff substrates, which was experimentally determined. If pNF_0 is set to 1, *pNF* can be expressed simply as the fold change from the baseline (1.0). Thus,

$$pNF = pNF_m \frac{1 - e^{-\alpha_{pNF}t}}{1 + (1 - e^{\alpha_I t})(R - 1)} + e^{-\alpha_{pNF}t} \quad (Eq. 1.15).$$

Therefore, *I* affects *pNF* only via α_I.

R, pNF_m, α_I, and α_{pNF} were determined by fitting the experimental data to Eq. 1.15. Out of these parameters, fitting the data in **Fig. 2A** shows that only pNF_m (and thus pNF_{st}) is significantly different between soft and stiff substrates (**Fig. S2D**).

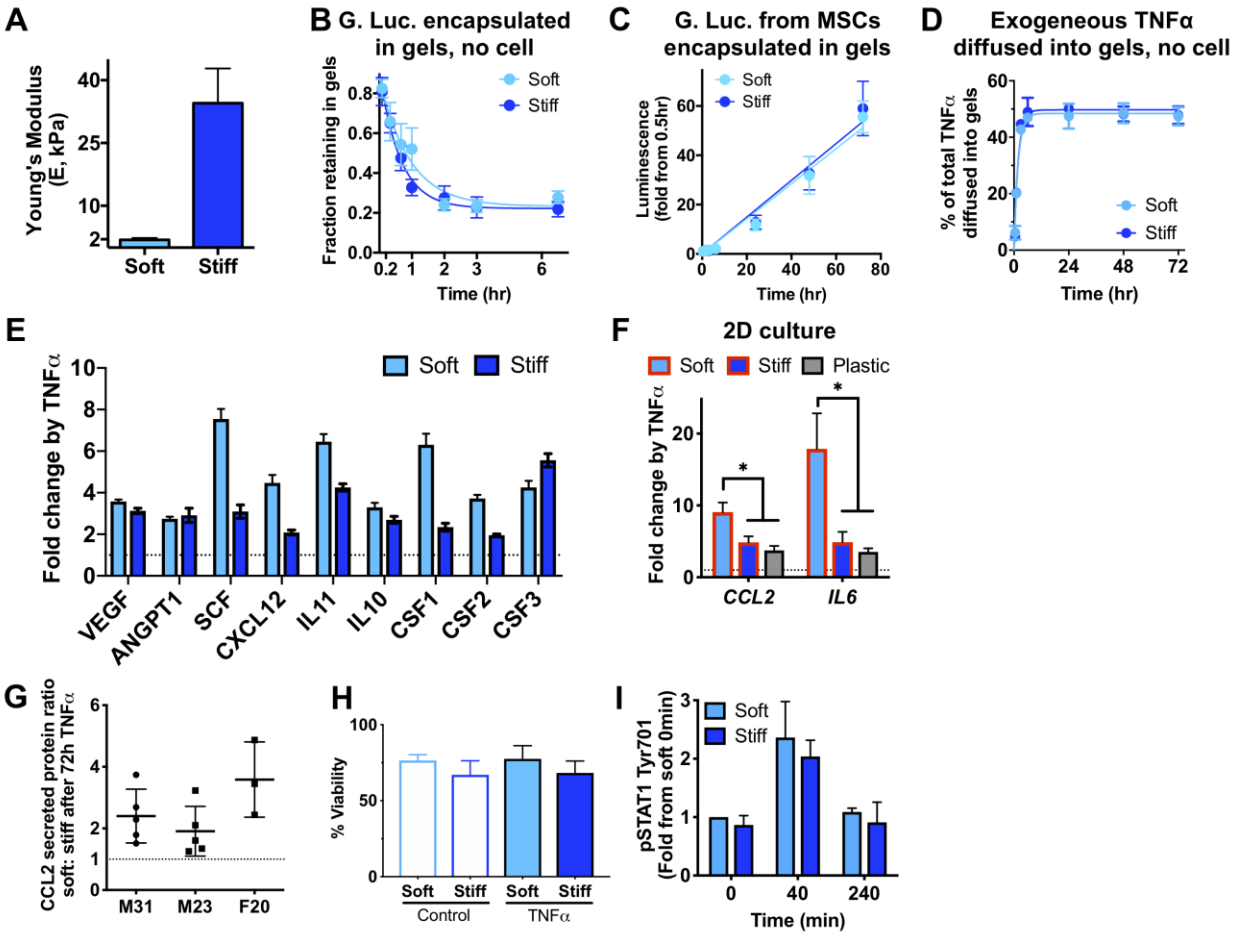

Figure S1. Characterization of soluble factor diffusion and response of MSCs to TNFα in engineered alginate hydrogels. (A) AFM was used to measure Young's modulus (*E*) of 'soft or 'stiff' alginate gels. Alginate hydrogels were formed by different calcium sulfate concentrations: 12~12.5 mM for soft (*E* ~2 kPa) and 35~40 mM for stiff (*E* ~ 35 kPa). Representative graphs from a batch of alginate-RGD. n ≥ 20 measurements. Error bars: ± SD. **(B)** Diffusion of *Gaussia luciferase* from ionic alginate hydrogels to media over time. The conditioned media from MSCs expressing *Gaussia luciferase* was mixed with alginate solutions to form soft or stiff gels, which were then punched into discs, followed by incubation in DMEM for 37°C. The gels were washed and digested into solutions by adding 50 mM EDTA at the indicated time points. The amount of *Gaussia luciferase* remaining in gels was normalized by that of total *Gaussia luciferase* encapsulated in gels. Half-time of protein diffusion = ~32 min for both soft and stiff gels. n = 3 technical replicates ± SD **(C)** Secretion kinetics of *Gaussia luciferase* from engineered MSCs in 3D alginate-RGD hydrogels. The media were collected at the indicated time points to measure the level of *Gaussia luciferase*. All the values were normalized by the signal at 30 min in culture.

Linear fit for both soft and stiff groups, slope = 0.7/hr. n = 3 experiments ± SEM. **(D)** Diffusion of exogenously added TNFα into soft or stiff alginate hydrogels. 100 ng/ml recombinant TNFα was added to soft or stiff gels and the amount of TNFα in gels at different time points was quantified by ELISA and normalized to total amount of TNFα added. One-phase association kinetics fit, $t_{1/2}$ = ~1.2hr, plateau = ~50% for both soft and stiff gels. n = 3 technical replicates ± SD. **(E)** Changes in mRNA expression of a panel of genes in response to treatment of TNFα for 3 days in soft or stiff gels. n = 3 technical replicates for each gene ± SD. **(F)** TNFα-induced upregulation of *CCL2* and *IL6* mRNAs in MSCs plated on 2D culture environments. For each gene, $P<0.05$ from one-way ANOVA with Tukey's HSD test, $^*P<0.05$ (n = 3 experiments). Error bars indicate ± SEM. **(G)** Fold difference in TNFα-induced CCL2 protein expression between MSCs in soft and stiff matrices across different donors. M/F: male or female; Number = age. Each data point is from an independent experiment (3~5 experiments per donor). **(H)** Percentage of viable (calcein positive, ethidium bromide negative) MSCs after encapsulation in soft or stiff 3D gels and culturing for 1 day. n = 3 experiments ± SEM. **(I)** Phosphorylation levels of STAT1 at Tyr701 in response to IFNγ in hydrogel-encapsulated MSCs evaluated by intracellular flow cytometry. n = 3 technical replicates ± SD.

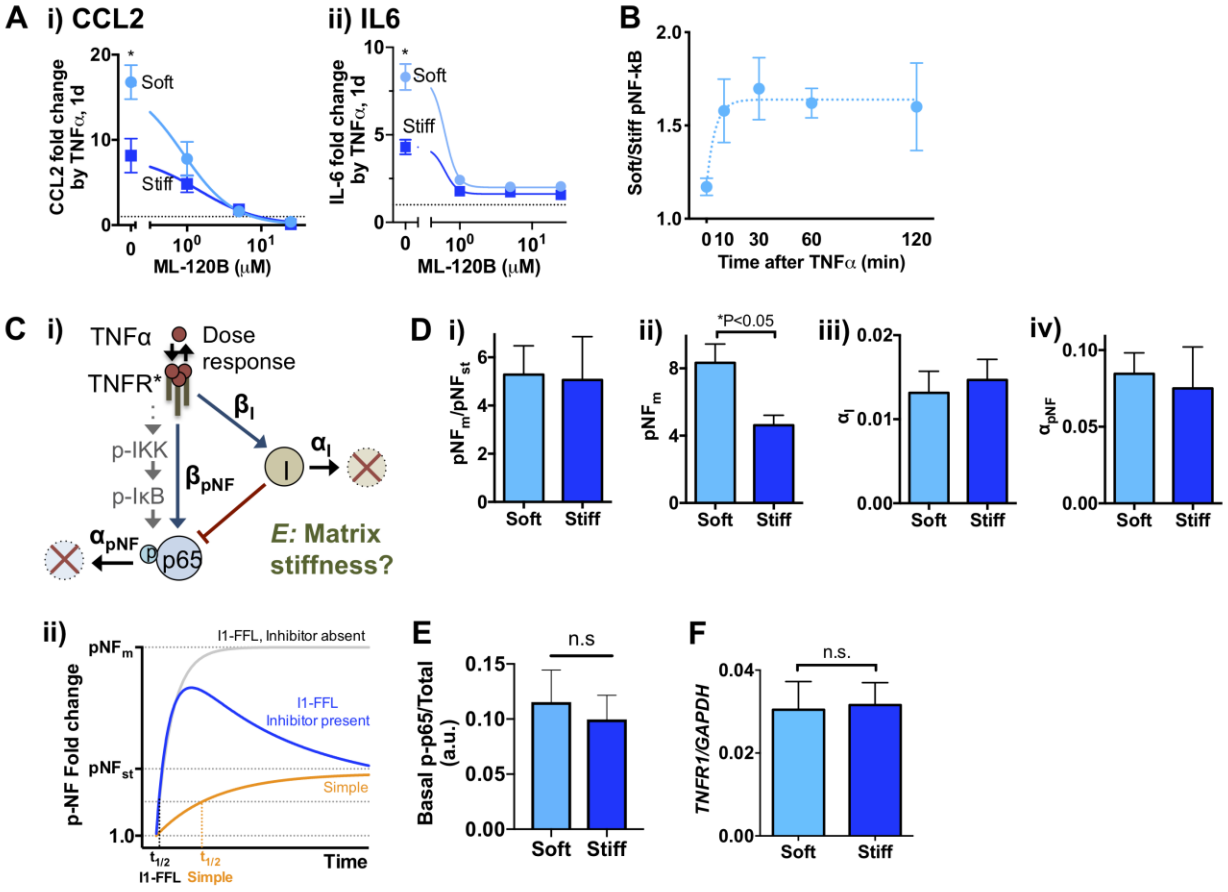

Figure S2. Characterization of TNFα-induced NF-κB activation kinetics and surface TNFR1 clustering in MSCs encapsulated in alginate-RGD hydrogels. (A) Upregulation of CCL2 and IL6 by TNFα requires IKK. Dose-response curves are shown in response to the IKK2 selective inhibitor ML-120B for 1 day. (i) CCL2, soft IC50 ~ 0.9 μM and stiff IC50 ~ 1.4 μM with Hill coefficient ~1.0 for both soft and stiff. (ii) IL6, IC50 ~ 0.6 μM with Hill coefficient ~1.5 for both soft and stiff. Paired T-test, *P<0.05 soft *vs.* stiff at each dose. n = 3 experiments ± SEM. **(B)** Experimental results showing the ratio of activated NF-κB in MSCs between soft and stiff substrates at different time points. One phase association kinetics fit shows plateau = ~1.6 at t ≥ 10 min. n = 3 experiments ± SEM. **(C)** (i) A modeling scheme showing a pulse generator circuit. β_I, intrinsic rate of inhibitor activation; α_I, decay rate of inhibitors; β_{pNF}**,** intrinsic rate of p65 activation (combined steps including IKK activation (p-IKK) and IκB degradation (p-IκB)); α_{pNF}**,** decay rate of activated p65. These components form an incoherent feedforward loop (I1-FFL). (ii) A representative graph of the I1-FFL model. In the absence of the inhibitor, activated

NF-κB reaches the maximum level (pNF_m). In the presence of the inhibitor, the I1-FFL model shows a pulse-like behavior where activation of NF-κB occurs rapidly followed by gradual deactivation, finally reaching the steady state (pNF_{st}). Compared to the simple regulation with the equivalent pNF_{st}, I1-FFL accelerates the response time ($t_{1/2}$). **(D)** Results from fitting the experimental data (**Fig. 2A**) to the I1-FFL based model. (i) pNF_m/pNF_{st}. (ii) pNF_m. (iii) The decay rate of the inhibitor (α_I). (iv) The decay rate of the activated NF-κB (α_{pNF}). n = 3 experiments ± SEM. **(E)** The basal level of phosphorylated NF-κB at Ser536 (p-p65) normalized to total p65. n = 3 experiments ± SEM. **(F)** Gene expression of *TNFR1* relative to *GAPDH* measured by qPCR. n = 3 technical replicates ± SD.

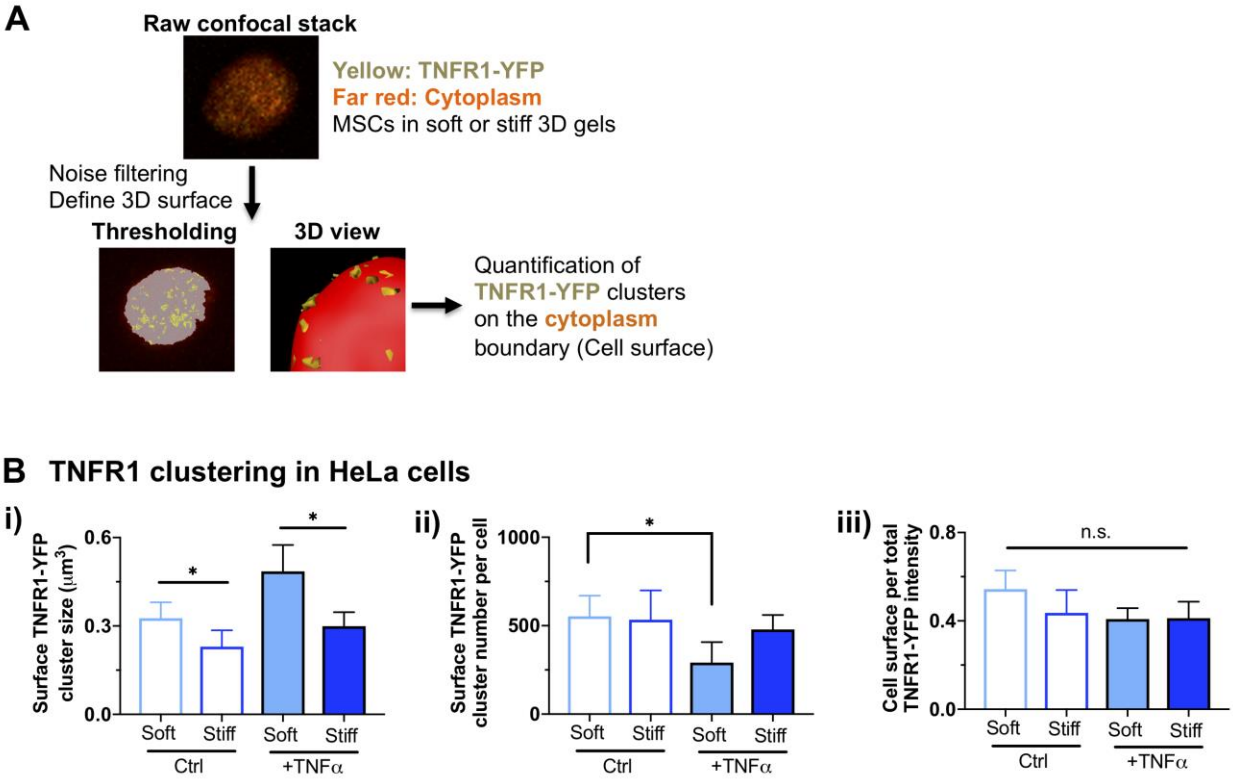

Figure S3. Characterization of TNFR1 clustering as a function of matrix stiffness. (A) An overview of the method to quantify cell surface clusters of TNFR1-YFP by using confocal imaging and image processing (see **Methods**). **(B)** Cell surface distribution and clustering of TNFR1-YFP in HeLa cells encapsulated in soft or stiff 3D gels. (i) Cluster size of TNFR1-YFP on the cell surface. (ii) Cluster number of TNFR1-YFP per cell. (iii) Cell surface per total TNFR1-YFP intensity. $P<0.05$ One-way Brown-Forsythe and Welch ANOVA for i and ii with Dunnett T3 multiple comparisons test, $^*P<0.05$ (n = 15 cells from 2 experiments). Error bars: ± SD.

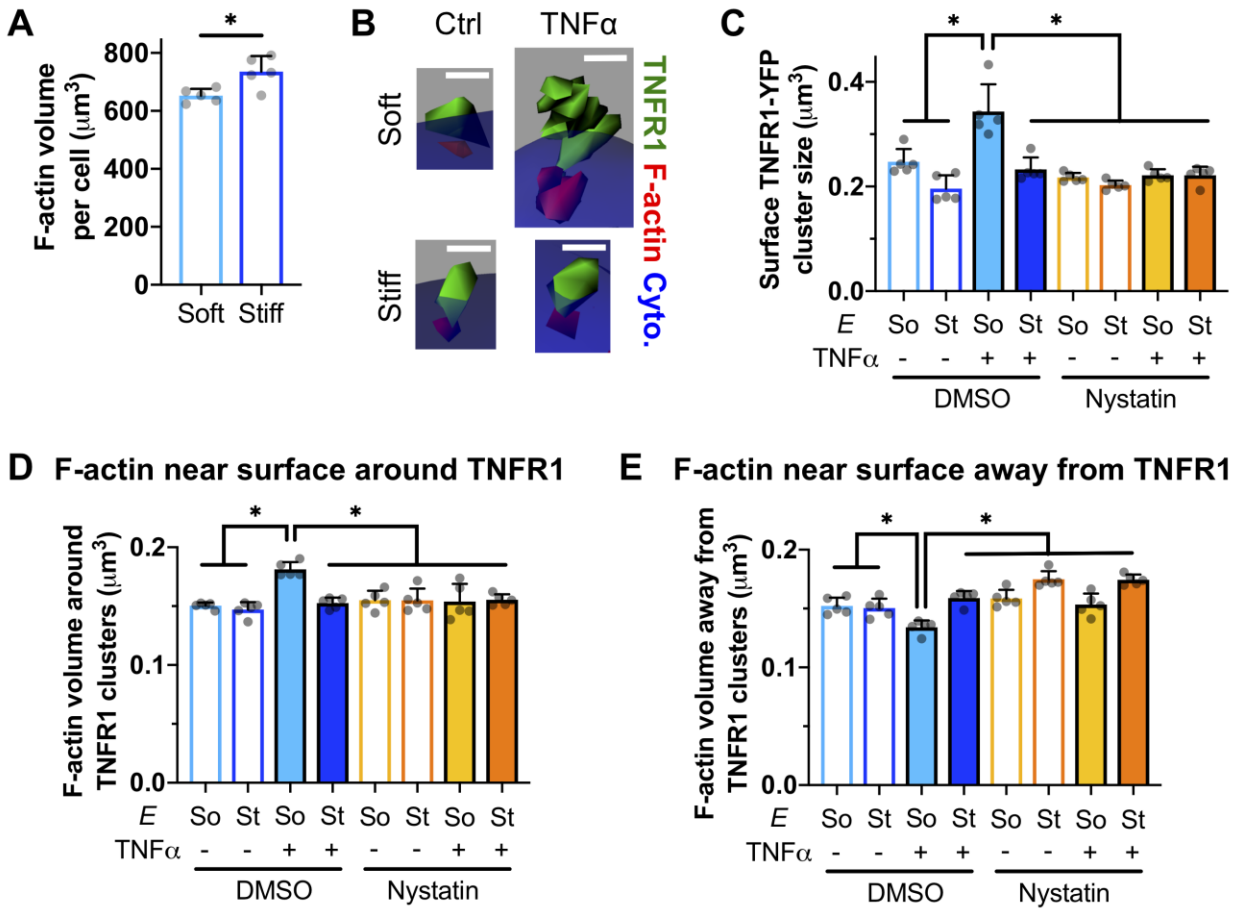

Figure S4. Characterization of TNFR1 and F-actin near the cell surface as a function of matrix stiffness and lipid rafts. (A) Total F-actin volume per cell in soft *vs.* stiff matrix measured by quantifying LifeAct-RFP signals from 3D reconstructed confocal images. Unpaired T-test, *P<0.05 soft *vs.* stiff (n = 5 cells from 2 experiments). Error bars: ± SD. **(B)** Representative confocal images from 3D construction showing TNFR1-YFP (green) on the outer boundary of the cytoplasm (CellTrace, blue), along with F-actin (LifeAct-RFP, red) adjacent to TNFR1-YFP. Scale bar = 0.5 μm. **(C)** Cluster size of TNFR1-YFP on the cell surface as a function of matrix stiffness, TNFα, and nystatin. Labeled MSCs in soft or stiff gels were preincubated with either DMSO or nystatin (50 μM) for 2 hours, followed by treatment with or without TNFα (100 ng/ml) for 20 min prior to confocal imaging (see **Methods**). **(D)** F-actin volume at the vicinity (within 2-μm^3) of TNFR1-YFP on the cell surface. (**E**) F-actin volume around the cell surface where TNFR1-YFP is not visible. For (C)-(E), P<0.05 from one-way ANOVA with Tukey's HSD test, *P<0.05 (n = 5 cells from 2 experiments, the mean value of each cell from at least 70 measurements). Error bars: ± SD.

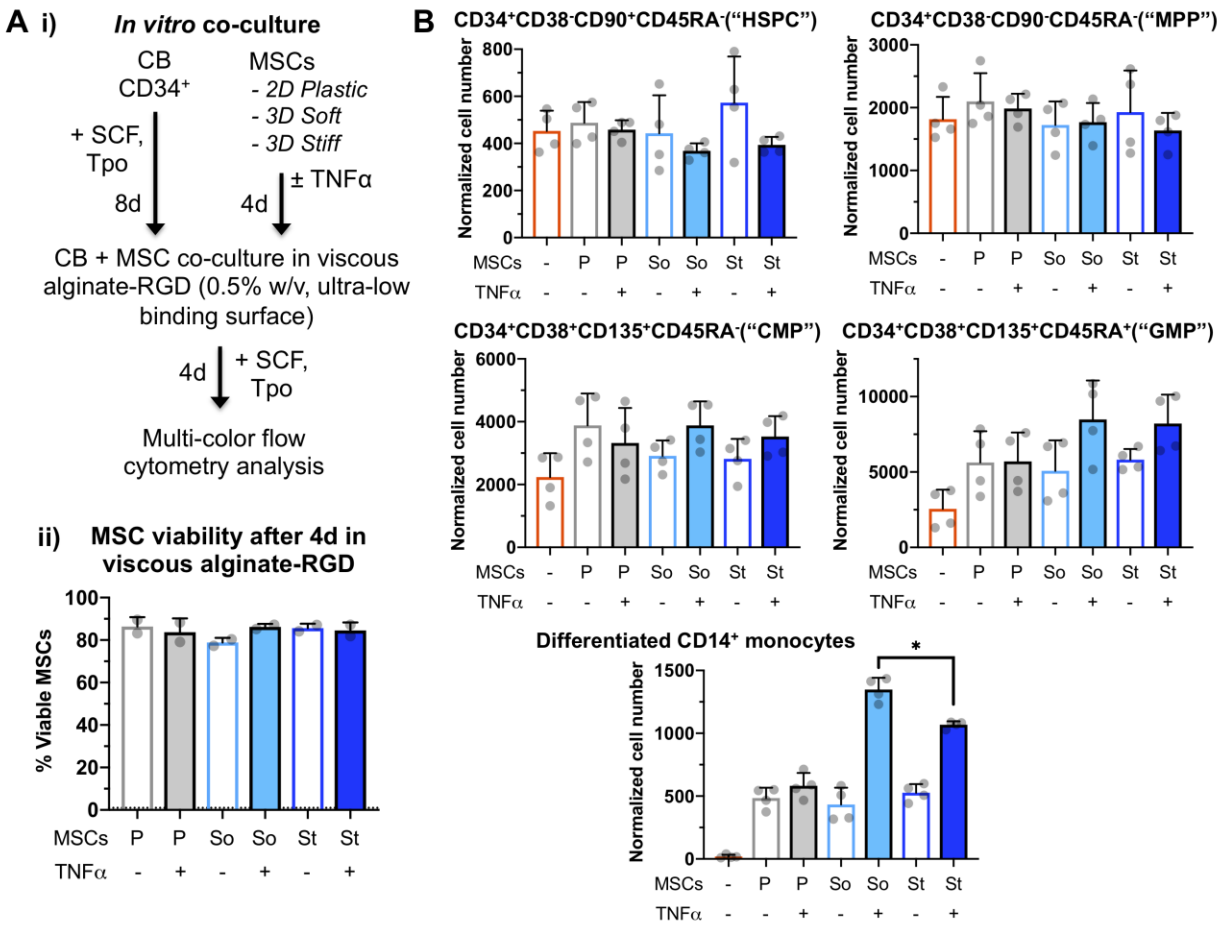

Figure S5. Effects of different culture environments on the ability of MSCs to impact hematopoiesis *in vitro*. (A) (i) Experimental Scheme (see **Methods**). CB: Cord Blood, SCF: Stem Cell Factor, Tpo: Thrombopoietin. (ii) Viability of primed MSCs after culturing in the alginate-RGD fluid (0.5% w/v) without gelation for 4 days. n = 2 technical replicates ± SD. **(B)** Quantification of different hematopoietic cell populations evaluated by multicolor flow cytometry. The indicated surface marker phenotypes are based on previous studies on human hematopoiesis (*33*, *34*). HSPC: Early hematopoietic stem progenitor cell, MPP: Multipotent progenitor, CMP: Common myeloid progenitor, GMP: granulocyte/monocyte progenitor. Cell number for each subpopulation was normalized to 5000 total CB cells precultured for 8 days prior to co-culture. For GMP and differentiated $CD14^+$ monocytes, $P<0.05$ from one-way Brown-Forsythe and Welch ANOVA with Dunnett T3 multiple comparisons test, $^*P<0.05$ (n = 4 pooled from 2 experiments). Error bars: ± SD.

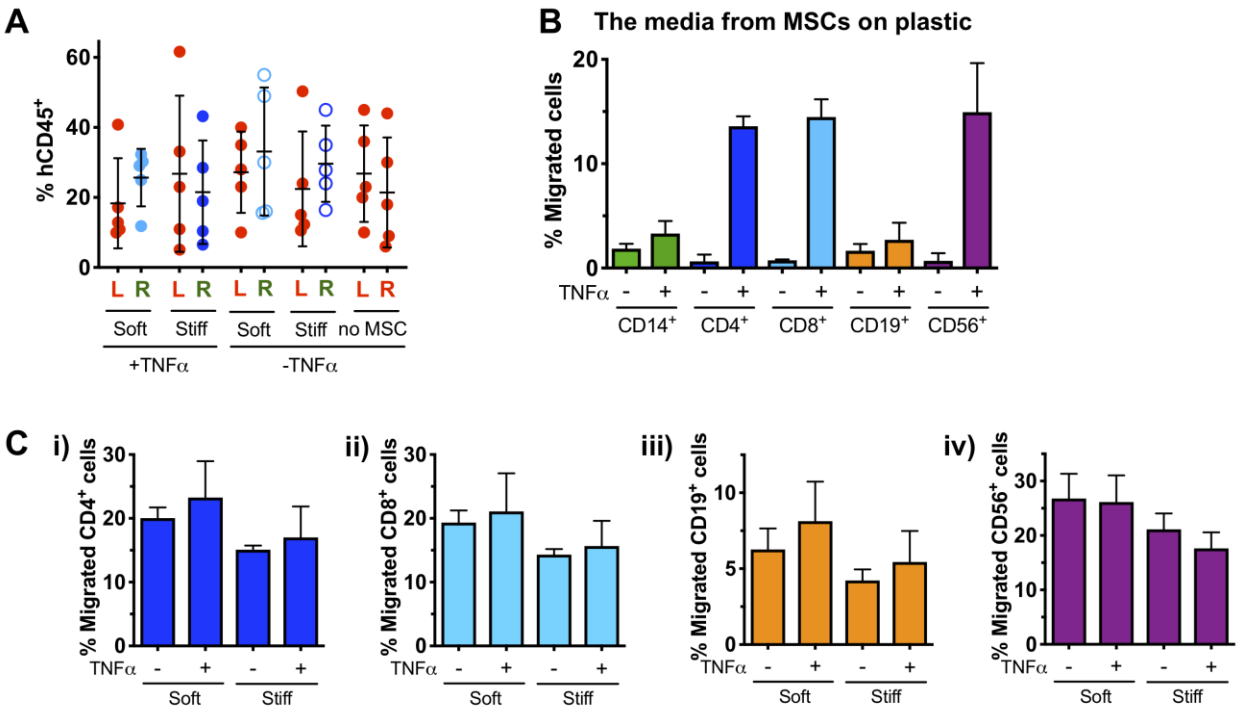

Figure S6. Characterization of human hematopoietic engraftment and chemotaxis. (A) Percentage of human $CD45^+$ ($hCD45^+$) cells in tibias relative to total $CD45^+$ cells (mouse $CD45^+$ cells and human $CD45^+$ cells). The analyses were done 4 days after PBS was delivered to the left tibia, and MSCs were delivered to the right tibia. n = 5 recipients from 2 independent experiments. **(B)** Percentage of migrated human peripheral mononuclear blood cell lineages towards the conditioned media from MSCs on plastic ± TNFα. n = 2 experiments ± SD. **(C)** The extent of lymphoid cell migration under chemotactic gradient through 3-μm pores for 3 hours. (i) $CD4^+$ cells. (ii) $CD8^+$ cells. (iii) $CD19^+$ cells. (iv) $CD56^+$ cells. n = 3 experiments ± SEM.

Table S1. List of primers for qPCR analysis

Gene (human)	Sequence (5' → 3')
CCL2	F: AAGATCTCAGTGCAGAGGCTCG R: TTGCTTGTCCAGGTGGTCCAT
CCL7	F: GAGAGCTACAGAAGGACCAC R: GTTTTCTTGTCCAGGTGCTTC
IL6	F: GGTACATCCTCGACGGCATCT R: GTGCCTCTTTGCTGCTTTCAC
IL8	F: ACTGAGAGTGATTGAGAGTGGAC R: AACCCTCTGCACCCAGTTTTC
TSG6	F: AATACAAGCTCACCTACGCAG R: GGTATCCAACTCTGCCCTTAG
TNFR1	F: TGCCAGGAGAAACAGAACAC R: TCCTCAGTGCCCTTAACATTC
CAV1	F: CCTTCCTCAGTTCCCTTAAAGC R: TGTAGATGTTGCCCTGTTCC
ANGPT1	F: AACCGAGCCTATTCACAGTATG R: ATCAGCACCGTGTAAGATCAG
CSF1	F: CGCTTCAGAGATAACACCCC R: TCATAGAAAGTTCGGACGCAG
CSF2	F: CTGAACCTGAGTAGAGACACTG R: GCCCTTGAGCTTGGTGAG
CSF3	F: TTCCTGCTCAAGTGCTTAGAG R: AGCTTGTAGGTGGCACAC
CXCL12	F: ACTCCAAACTGTGCCCTTC R: GACCCTCTCACATCTTGAACC
IL10	F: CGCATGTGAACTCCCTGG R: TAGATGCCTTTCTCTTGGAGC
IL11	F: CGGACAGGGAAGGGTTAAAG R: CACAGGCTCAGCACGAC
SCF	F: CCAGAACAGCTAAACGGAGTC R: GACGAGAGGATTAAATAGGAGCAG
VEGF	F: AGTCCAACATCACCATGCAG R: TTCCCTTTCCTCGAACTGATTT